Title
Clinical efficacy of a RAF inhibitor needs broad target blockade in BRAF-mutant melanoma.

Journal
Nature, 467(7315)

ISSN
0028-0836

Authors
Bollag, Gideon
Hirth, Peter
Tsai, James
et al.

Publication Date
2010-09-01

DOI
10.1038/nature09454

Peer reviewed

HHS Public Access

Author manuscript

Nature. Author manuscript; available in PMC 2011 March 30.

Published in final edited form as:

Nature. 2010 September 30; 467(7315): 596–599. doi:10.1038/nature09454.

Clinical efficacy of a RAF inhibitor needs broad target blockade in *BRAF*-mutant melanoma

Gideon Bollag[*], **Peter Hirth**[*], **James Tsai**[*], **Jiazhong Zhang**[*], **Prabha N. Ibrahim**[*], **Hanna Cho**[*], **Wayne Spevak**[*], **Chao Zhang**[*], **Ying Zhang**[*], **Gaston Habets**[*], **Elizabeth A. Burton**[*], **Bernice Wong**[*], **Garson Tsang**[*], **Brian L. West**[*], **Ben Powell**[*], **Rafe Shellooe**[*], **Adhirai Marimuthu**[*], **Hoa Nguyen**[*], **Kam Y. J. Zhang**[*], **Dean R. Artis**[*], **Joseph Schlessinger**[@], **Fei Su**[$], **Brian Higgins**[$], **Raman Iyer**[$], **Kurt D'Andrea**[#], **Astrid Koehler**[$], **Michael Stumm**[$], **Paul S. Lin**[*], **Richard J. Lee**[$], **Joseph Grippo**[$], **Igor Puzanov**[%], **Kevin B. Kim**[^], **Antoni Ribas**[&], **Grant A. McArthur**[+], **Jeffrey A. Sosman**[%], **Paul B. Chapman**[α], **Keith T. Flaherty**[#], **Xiaowei Xu**[†], **Katherine L. Nathanson**[#], and **Keith Nolop**[*]

[*]Plexxikon Inc.

[@]Yale University

[$]Roche Pharmaceuticals

[#]Department of Medicine, Abramson Cancer Center, University of Pennsylvania

[†]Department of Pathology and Laboratory Medicine, Abramson Cancer Center, University of Pennsylvania

[%]Vanderbilt University

[^]The University of Texas M. D. Anderson Cancer Center

[&]University of California, Los Angeles

[+]Peter MacCallum Cancer Centre

[α]Memorial Sloan Kettering Cancer Center

Abstract

B-RAF is the most frequently mutated protein kinase in human cancers.1 The finding that oncogenic mutations in *BRAF* are common in melanoma2 followed by the demonstration that

Reprint requests to: Gideon Bollag, PhD Plexxikon Inc. 91 Bolivar Dr. Berkeley, CA 94710 gbollag@plexxikon.com.

Supplementary Information will be linked to the online version of the paper at www.nature.com/nature.

Author Contributions

GB, PH, CZ, KLN, and KN designed studies, interpreted data and wrote the manuscript. JT, GH, EAB, BW, GT, BLW, BP, RS, AM, HN, FS, and BH conducted or managed biochemical or biological studies. JZ, PNI, HC, WS, DRA and RI designed and conducted chemistry and formulation experiments. YZ and KYJZ conducted and interpreted structural studies. JS helped interpret data and write the manuscript. KD, AK, MS, and XX designed, managed and interpreted biomarker studies. PSL, RJL, JG, IP, KBK, AR, GAM, JAS, PBC and KTF managed or conducted clinical and translational studies.

Author Information

Atomic and structural data have been deposited in Protein Data Bank under accession number 3OG7. Many of the authors are employed by the biotechnology company Plexxikon or the pharmaceutical company Roche, as indicated in the author affiliations.

these tumors are dependent on the RAF/MEK/ERK pathway3 offered hope that inhibition of B-RAF kinase activity could benefit melanoma patients. Herein, we describe the structure-guided discovery of PLX4032 (RG7204), a potent inhibitor of oncogenic B-RAF kinase activity. Preclinical experiments demonstrated that PLX4032 selectively blocked the RAF/MEK/ERK pathway in *BRAF* mutant cells and caused regression of *BRAF* mutant xenografts.4 Toxicology studies confirmed a wide safety margin consistent with the high degree of selectivity, enabling Phase 1 clinical trials using a crystalline formulation of PLX4032.5 In a subset of melanoma patients, pathway inhibition was monitored in paired biopsy specimens collected before treatment initiation and following two weeks of treatment. This analysis revealed substantial inhibition of ERK phosphorylation, yet clinical evaluation did not show tumor regressions. At higher drug exposures afforded by a new amorphous drug formulation,4,5 greater than 80% inhibition of ERK phosphorylation in the tumors of patients correlated with clinical response. Indeed, the Phase 1 clinical data revealed a remarkably high 81% response rate in metastatic melanoma patients treated at an oral dose of 960 mg twice daily.5 These data demonstrate that *BRAF*-mutant melanomas are highly dependent on B-RAF kinase activity.

Keywords

BRAF; melanoma; PLX4032; biomarker; oncogene; targeted therapy

---

PLX4032 belongs to a family of mutant B-RAF kinase inhibitors discovered using a scaffold-based drug design approach.6 The crystallography-guided approach allowed optimization of a compound with modest preference for the mutated form of B-RAF (B-RAF^{V600E}) in comparison to wild-type B-RAF. Supplementary Table 1 summarizes the differential ability for PLX4032 to inhibit the activity of over 200 kinases. PLX4032 displays similar potency for B-RAF^{V600E} (31nM) and c-RAF-1 (48nM) and selectivity against many other kinases, including wild type B-RAF (100nM). While the vast majority of kinases are minimally affected, several were found that were also inhibited at <100 nM concentrations in biochemical assays; to date, inhibition of these non-RAF kinases such as ACK1, KHS1 and SRMS has not been tested in cellular assays. As previously demonstrated for the related B-RAF inhibitor PLX4720,6 the biochemical selectivity of PLX4032 translates to cellular selectivity: potent inhibition of ERK phosphorylation and proliferation occurs exclusively in *BRAF*-mutant cell lines.4

PLX4032 was crystallized with a protein construct that contained the kinase domain of B-RAF^{V600E}.PLX4032 (Figure 1A) binds in the active site of one of the protomers in the non-crystallographic-symmetry related dimer (Figure 1). As previously described for the related RAF inhibitor PLX4720 (PDB ID: 3C4C),6 the PLX4032-bound protomer adopts the DFG-in conformation to enable the formation of a unique hydrogen bond between the backbone NH of Asp^{594} and the sulfonamide nitrogen of PLX4032 (Figure 1B). In addition, PLX4032-binding causes an outward shift in the regulatory αC helix, which may explain why the effect of PLX4720 and PLX4032 on RAF dimerization is so different from other RAF inhibitors such as AZD-628 and GDC-0879 (Figure 1C).7 The apo-protomer displays the DFG-in conformation with the activation loop locked away from the ATP-binding site by a salt-bridge between Glu^{600} and Lys^{507} (Figure 1D).

In *BRAF*^{V600E}-mutant xenograft studies, PLX4032 demonstrated dose-dependent inhibition of tumor growth, with higher exposures resulting in tumor regression (Figure 2A and reference 4). Efficacy could be demonstrated in cell lines and xenografts bearing either homozygous or heterozygous *BRAF* mutations. By contrast, no effect was observed on melanoma xenograft growth if both *BRAF* alleles were wild-type.4,6 Due to their consistent pharmacokinetics in rodents, PLX4032 and PLX4720 were prioritized over a panel of related compounds that all displayed similar activities *in vitro* and *in vivo*. For further drug development, PLX4032 was chosen (over PLX4720) because its pharmacokinetic properties scaled appropriately in beagle dogs and cynomolgus monkeys.

In order to estimate PLX4032 exposures (as defined by AUC $_{0\text{-}24}$, the Area Under the plasma Concentration time curve over the dosing period of 24 hours) that correlated with tumor response, conventionally formulated daily oral doses of PLX4032 were administered in the *BRAF*^{V600E}-bearing colorectal cancer COLO205 xenograft model. In this model, tumor growth inhibition was modest at 6 mg/kg (AUC $_{0\text{-}24}$ ~ 50 μM*hr), tumor stabilization was seen at 20 mg/kg (AUC $_{0\text{-}24}$ ~ 200 μM*hr), and significant tumor regressions were observed at 20 mg/kg BID (AUC $_{0\text{-}24}$ ~ 300 μM*hr). *BRAF*^{V600E}-bearing melanoma xenograft models, including NCI-LOX and COLO829 are also sensitive to PLX4032.4

Rats and beagle dogs were dosed for 28 days with increasing doses up to 1000 mg/kg/day, and no toxicity was detected at any dose level. Likewise, no adverse effects were detected in a standard battery of safety pharmacology studies. Subsequent toxicology studies of longer duration, 26 weeks in rats and 13 weeks in dogs, further confirmed the tolerability of the compound. This safety profile was achieved in spite of very high compound exposures, reaching 2600 μM*h in rats and 820 μM*h in dogs. The rat exposures exceeded those that were effective in patients (see below). Importantly, no histological changes were observed in the skin in any animal at any dose or duration of treatment, contrasting to results observed with other RAF inhibitors.7

These preclinical findings provided the necessary support in order to initiate Phase 1 clinical testing in cancer patients. Clinical and pharmacokinetic results from this Phase 1 study recently have been reported.5 In the initial stage of the Phase 1 study, cohorts of patients with advanced solid tumors were treated with escalating doses of PLX4032 (ranging from 200 to 1600 mg), administered twice-daily as oral capsules. The initial crystalline formulation yielded modest drug exposures, so PLX4032 was reformulated as a microprecipitated bulk powder (MBP) and doses ranging from 160 to 1120 mg BID were sequentially evaluated. Preclinical experiments in mice (Figure 2B and reference 4) and dogs demonstrated that the MBP formulation substantially increased drug bioavailability by ten-fold. This improved bioavailability also was observed in patients, with mean exposures at a 160 mg BID dose of the MBP formulation (day 15 AUC $_{0\text{-}24}$ = 185 μM·h) similar to a 1600 mg BID dose of the original formulation (day 15 AUC $_{0\text{-}24}$ = 203 μM·h).

During the dose-escalation phase of the clinical trial, twenty-one patients with metastatic melanoma, sixteen with and five without *BRAF*-mutations, were treated at doses that achieved AUC $_{0\text{-}24}$ > 300 μM·h.5 Tumor dimensions were measured by computed tomography (CT). Ten patients with *BRAF*-mutant melanoma achieved tumor regressions

qualifying as partial responses (PR, by Response Evaluation Criteria in Solid Tumors [RECIST 1.0], >30% reduction in tumor dimensions) and one patient had a complete response (CR); none of the patients with melanomas lacking *BRAF* mutations achieved PR. These data along with preclinical evidence of selectivity for *BRAF*-mutant cell lines strongly justified limiting all further enrollment to patients with *BRAF*-mutant tumors. Dose-limiting toxicities detected at the 1120 mg BID dose included fatigue, rash, and joint pain.5 Therefore, 960 mg BID was identified as the maximum tolerated dose (MTD), and a cohort of 32 patients with *BRAF*-mutant melanoma was enrolled at this dose in an extension of the Phase 1 study.

At the 960 mg BID dose, the steady state PLX4032 concentration was 86 μM and the $AUC_{0\text{-}24}$ was 1741 μM·h; the half-life was estimated to be 50 hours.5 Out of the 32 patients treated at this dose, 24 experienced tumor regressions qualifying as PRs and two patients had CRs. $BRAF^{V600E}$ mutation status was assessed by a real-time polymerase chain reaction (PCR) assay as described under methods,5,8 and many of the samples were sequenced for verification of the PCR result. The reliability of the PCR assay is currently being assessed in concurrent Phase 2 and Phase 3 trials. The $BRAF^{V600E}$ allele was detected in 46 of the 48 *BRAF*-positive patients described above. Interestingly, subsequent sequencing revealed that tumors from the two patients lacking the $BRAF^{V600E}$ mutation were found to carry the $BRAF^{V600K}$ mutation and were among the better responders (71% and 100% reduction in tumor dimensions); and an additional $BRAF^{V600K}$ response has been recently published.9

During the dose escalation stage of the study, a cohort of patients had paired tumor biopsies to evaluate pathway inhibition, one taken prior to initiation of PLX4032 treatment and the second taken after 14 days of PLX4032 treatment. Patients on the paired biopsy cohort varied widely in plasma exposures. In addition to expected inter-patient variability in drug clearance, these patients were treated at different doses and with the two different formulations (one crystalline and one amorphous). To monitor ERK pathway activity, phosphorylated-ERK (pERK) levels were determined by immunohistochemistry (IHC), both in the nucleus and in the cytoplasm. To monitor proliferation, Ki67 levels also were measured.

As shown in Supplementary Table 2, levels of pERK and Ki67 were decreased in most biopsies following two weeks of dosing with PLX4032, even in patients with modest drug exposure. Patients exposed to plasma levels of PLX4032 less than 300 μM·h experienced no measurable decreases in tumor burden. In contrast, patients exposed to higher plasma levels of PLX4032 experienced tumor regression, often achieving PRs as defined by RECIST criteria (Supplementary Table 2). Representative pictures illustrating decreases in ERK phosphorylation and Ki67 are shown in Figures 3A and 3B. Interestingly, decreases in cytoplasmic pERK correlated well with tumor response (Figure 3C), while changes in nuclear pERK correlated poorly (Figure 3D). In general nuclear pERK was more sensitive to compound levels than cytoplasmic pERK, consistent with the idea that nuclear ERK responds very quickly to phosphorylation/dephosphorylation events, while cytoplasmic ERK phospho-events are buffered by the many cytoplasmic scaffolding proteins. As further evidenced in Supplementary Table 2, the improved pathway inhibition and tumor responses correlate with higher plasma drug exposures. In patients with tumor regressions, pathway

analysis typically showed greater than 80% inhibition of cytoplasmic ERK phosphorylation (Figure 3C). This result indicates that near-complete inhibition of ERK signaling may be needed for significant tumor response.

A growing body of literature shows that oncogenic BRAF is an important stimulator of metabolic activity,10,11 and in preclinical studies PLX4032 rapidly inhibits fluoro-deoxy-glucose (FDG) uptake specifically in $BRAF^{V600E}$ mutant melanoma cell lines.12 Therefore, FDG uptake in patients on the PLX4032 trial was assessed using PET imaging before treatment and following two weeks of dosing. All of the assessable patients treated with MBP-formulated PLX4032 experienced major reductions in FDG uptake. Representative FDG-PET images are shown in Fig. 4.

Toxicities such as fatigue, rash, and joint pain in the treated patients are detailed separately.5 Thirty-one percent of the patients treated at the MTD developed skin lesions described as cutaneous squamous cell carcinomas, keratoacanthoma type.5 This toxicity is of particular interest, since investigators studying three other RAF inhibitors, sorafenib13-15, XL28116 and GSK211843617 also have noted these skin lesions in a subset of treated patients. While the occurrence of these treatment-emergent tumors warrants careful dermatological monitoring of patients during PLX4032 treatment, it should be noted that these lesions were resected, and no patients discontinued PLX4032 due to this toxicity.5 These skin lesions generally appear within a few months of treatment initiation in sun-exposed areas of skin, suggesting that pre-existing oncogenic mutations may potentiate the RAF inhibitor effects.

Recent publications suggest a potential mechanism that may in part account for the keratinocyte proliferation noted in the patients on study.7,18,19 These reports follow-up on prior descriptions of paradoxical activation of the RAF/MEK/ERK pathway by RAF kinase inhibitors.20-22 Current evidence suggests that wild-type RAF kinase activity can be activated by RAF dimerization.23 RAF dimerization can be induced by RAF inhibitors: binding to one protomer – while inhibiting the kinase activity of that protomer – concurrently induces a conformational switch in the partner protomer via an undefined allosteric mechanism to activate RAF kinase activity.7,19 This paradoxical activation occurs in cells in which RAS is activated either by mutation or by some other priming event. Modulation of RAF dimerization may not be the only unexpected effects of RAF inhibitors, since multiple additional factors are involved in both positive (e.g. KSR, SRC, CNK) and negative (e.g. ERK, 14-3-3, DUSP, RKIP, RASSF) regulation of the RAF/MEK/ERK signaling pathway.24 25

The ability of PLX4032 to cause tumor regression in a large proportion of patients with *BRAF*-mutant advanced melanoma provides strong support for the hypothesis that the oncogenic B-RAF protein is a dominant driver of tumor growth and maintenance. These results are particularly interesting in that the *BRAF* mutation is likely an initiating event in melanoma tumorigenesis: the vast majority of benign nevi harbor the same $BRAF^{V600E}$ mutation.26 Our current understanding of melanocyte biology suggests that the nevi are benign because the *BRAF* mutation alone induces senescence.27 Clinical evaluation of sporadic nevi in patients treated at therapeutic doses revealed no effect of PLX4032 on nevi progression or regression.

The durability of response to PLX4032 is still under evaluation. Median progression free survival (PFS) in the Phase 1 extension cohort has not been reached but is currently estimated to be at least seven months.5 While this compares rather favorably with a PFS of less than two months in historical analysis of large numbers of advanced melanoma patients, 28 tumor re-growth occurs in many of the patients and the mechanisms of resistance are currently under investigation. Therefore, improved durability of response will be an important goal of further clinical trials. PLX4032 has the potential to anchor future treatments in combination with other targeted agents, immunotherapies, or chemotherapies and may thereby offer improved treatment options for *BRAF*-mutant melanoma patients.

METHODS SUMMARY

PLX4032 was synthesized using the general procedures previously described.6 Expression and purification of B-RAF, structure determination, protein kinase activity measurements, and xenograft studies were carried out as previously described.6 Clinical methods have also been recently described.5 Melanoma patients were selected for study using previously described TaqMan® methodology.8 Semi-quantitative immunohistochemistry for pERK and Ki67 was performed on 5 μm-thick formalin-fixed paraffin-embedded tumor biopsies following H&E staining to determine pathologic diagnosis and tissue morphology and integrity. The degree of phospho-ERK staining in the nucleus and cytoplasm was interpreted semiquantitatively by assessing the intensity and extent of staining on the slides. For Ki67 staining, the percentage of positive cells was determined.

Supplementary Material

Refer to Web version on PubMed Central for supplementary material.

Acknowledgements

We thank L Andries and M Knaapen from HistoGeneX for evaluating paired biopsies, and also our colleagues at the Molecular Imaging Research division of Charles River Labs for conducting the xenograft studies. We also thank D Heimbrook, S Cheng, L Burdette and B Lestini for helpful comments on the manuscript. This research was funded in part by NIH grants to KLN.

REFERENCES

1. Greenman C, et al. Patterns of somatic mutation in human cancer genomes. Nature. 2007; 446:153–158. [PubMed: 17344846]
2. Davies H, et al. Mutations of the BRAF gene in human cancer. Nature. 2002; 417:949–954. [PubMed: 12068308]
3. Solit DB, et al. BRAF mutation predicts sensitivity to MEK inhibition. Nature. 2006; 439:358–362. [PubMed: 16273091]
4. Yang H, et al. RG7204 (PLX4032), a selective BRAFV600E inhibitor, displays potent antitumor activity in preclinical melanoma models. Cancer Res. 2010; 70:5518–5527. [PubMed: 20551065]
5. Flaherty K, et al. Inhibition of Mutated, Activated BRAF in Metastatic Melanoma. N Engl J Med. 2010; 363:809–819. [PubMed: 20818844]
6. Tsai J, et al. Discovery of a selective inhibitor of oncogenic B-Raf kinase with potent antimelanoma activity. Proc Natl Acad Sci U S A. 2008; 105:3041–3046. [PubMed: 18287029]
7. Hatzivassiliou G, et al. RAF inhibitors prime wild-type RAF to activate the MAPK pathway and enhance growth. Nature. 2010

8. Koch WH. Technology platforms for pharmacogenomic diagnostic assays. Nature reviews. 2004; 3:749–761.
9. Rubinstein JC, et al. Incidence of the V600K mutation among melanoma patients with BRAF mutations, and potential therapeutic response to the specific BRAF inhibitor PLX4032. J Transl Med. 2010; 8:67. [PubMed: 20630094]
10. Esteve-Puig R, Canals F, Colome N, Merlino G, Recio JA. Uncoupling of the LKB1-AMPKalpha energy sensor pathway by growth factors and oncogenic BRAF. PloS one. 2009; 4:e4771. [PubMed: 19274086]
11. Zheng B, et al. Oncogenic B-RAF negatively regulates the tumor suppressor LKB1 to promote melanoma cell proliferation. Mol Cell. 2009; 33:237–247. [PubMed: 19187764]
12. Søndergaard JN, et al. Differential Sensitivity of Melanoma Cell Lines with BRAF V600E Mutation to the Specific B-Raf Inhibitor PLX4032. J Transl Med. 2010; 8:39. [PubMed: 20406486]
13. Arnault JP, et al. Keratoacanthomas and squamous cell carcinomas in patients receiving sorafenib. J Clin Oncol. 2009; 27:e59–61. [PubMed: 19597016]
14. Dubauskas Z, et al. Cutaneous squamous cell carcinoma and inflammation of actinic keratoses associated with sorafenib. Clin Genitourin Cancer. 2009; 7:20–23. [PubMed: 19213663]
15. Kong HH, et al. Keratoacanthomas associated with sorafenib therapy. J Am Acad Dermatol. 2007; 56:171–172. [PubMed: 17190642]
16. Schwartz GK, et al. A phase I study of XL281, a selective oral RAF kinase inhibitor, in patients (Pts) with advanced solid tumors. J Clin Oncol. 2009; 27:15s.
17. Kefford R, et al. Phase I/II study of GSK2118436, a selective inhibitor of oncogenic mutant BRAF kinase, in patients with metastatic melanoma and other solid tumors. J Clin Oncol. 2010; 28:8503.
18. Heidorn SJ, et al. Kinase-Dead BRAF and Oncogenic RAS Cooperate to Drive Tumor Progression through CRAF. Cell. 2010; 140:209–221. [PubMed: 20141835]
19. Poulikakos P, Zhang C, Bollag G, Shokat K, Rosen N. RAF inhibitors transactivate RAF dimers and ERK signaling in cells with wild-type BRAF. Nature. 2010; 464:427–430. [PubMed: 20179705]
20. Courtois-Cox S, et al. A negative feedback signaling network underlies oncogene-induced senescence. Cancer Cell. 2006; 10:459–472. [PubMed: 17157787]
21. Dougherty MK, et al. Regulation of Raf-1 by direct feedback phosphorylation. Mol Cell. 2005; 17:215–224. [PubMed: 15664191]
22. Hall-Jackson CA, et al. Paradoxical activation of Raf by a novel Raf inhibitor. Chem Biol. 1999; 6:559–568. [PubMed: 10421767]
23. Rajakulendran T, Sahmi M, Lefrancois M, Sicheri F, Therrien M. A dimerization-dependent mechanism drives RAF catalytic activation. Nature. 2009; 461:542–545. [PubMed: 19727074]
24. Pratilas CA, et al. (V600E)BRAF is associated with disabled feedback inhibition of RAF-MEK signaling and elevated transcriptional output of the pathway. Proc Natl Acad Sci U S A. 2009; 106:4519–4524. [PubMed: 19251651]
25. Kolch W. Coordinating ERK/MAPK signalling through scaffolds and inhibitors. Nat Rev Mol Cell Biol. 2005; 6:827–837. [PubMed: 16227978]
26. Pollock PM, et al. High frequency of BRAF mutations in nevi. Nat Genet. 2003; 33:19–20. [PubMed: 12447372]
27. Michaloglou C, et al. BRAFE600-associated senescence-like cell cycle arrest of human naevi. Nature. 2005; 436:720–724. [PubMed: 16079850]
28. Korn EL, et al. Meta-analysis of phase II cooperative group trials in metastatic stage IV melanoma to determine progression-free and overall survival benchmarks for future phase II trials. J Clin Oncol. 2008; 26:527–534. [PubMed: 18235113]

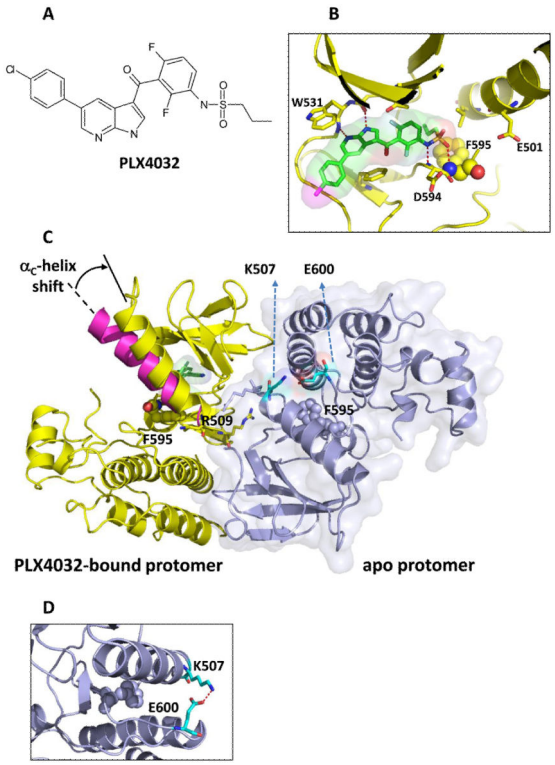

Fig 1. Three-dimensional structure of PLX4032 binding to B-RAF^{V600E}

A: The chemical structure of PLX4032.

B: Structure highlights the interactions of azaindole with the kinase hinge and the sulfonamide with the DFG loop, with F595 rendered in balls and other key protein residues shown as sticks.

C: The structure of the asymmetric dimer of B-RAF^{V600E} is shown with the PLX4032-protomer bound to PLX4032 colored yellow (consistent with panel B). The surface outline of the other protomer (blue) is shown lightly shaded. Highlighted residues are R509 to reflect its role in anchoring the dimer and F595 to show that both protomers are in the DFG-in state. The α_C-helix shown in magenta is overlaid on the PLX4032-bound protomer to show its typical configuration in an unoccupied protomer; the binding of PLX4032 causes a shift of the α_C-helix as noted by the arrow.

D. Magnified view of the salt bridge between Lys-507 and Glu-600 that helps prevent compound binding to the apo protomer.

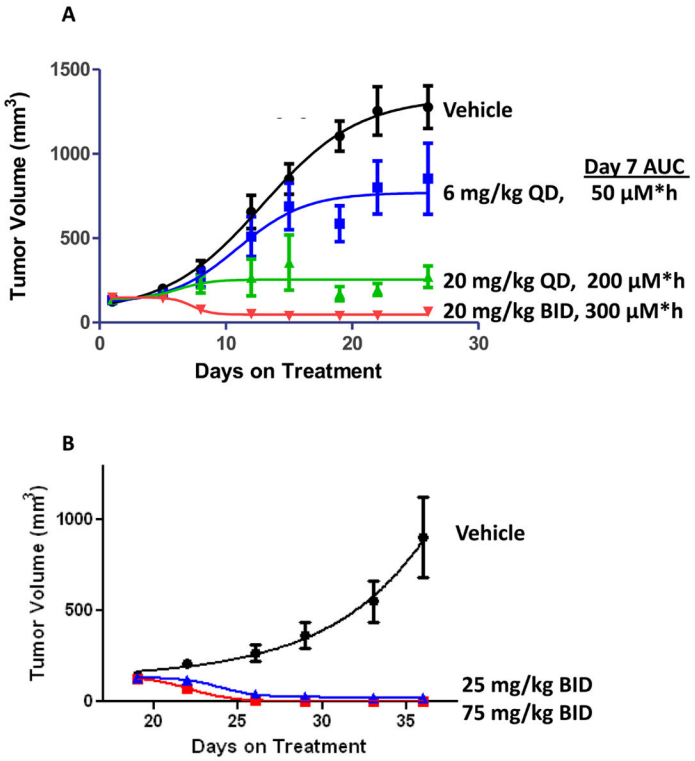

Fig 2. Effect of PLX4032 on COLO205 xenograft tumor growth

Tumor volume measurements of mice treated by oral gavage with the indicated doses of PLX4032 or vehicle (n=10 for all groups, error bars indicate standard error) are shown.

A. Administration in conventional formulation occurred daily. Exposures measured on day 7 are shown. At the 6, 20 and 20 BID doses, 1/10, 1/10, and 8/10 animals achieved CR, respectively.

B. Administration in the MBP formulation occurred twice daily. At the 25 mg/kg BID dose (blue), 7/10 animals achieved CR and 3/10 animals achieved PR; at the 75 mg/kg BID dose (red), all animals achieved CR.

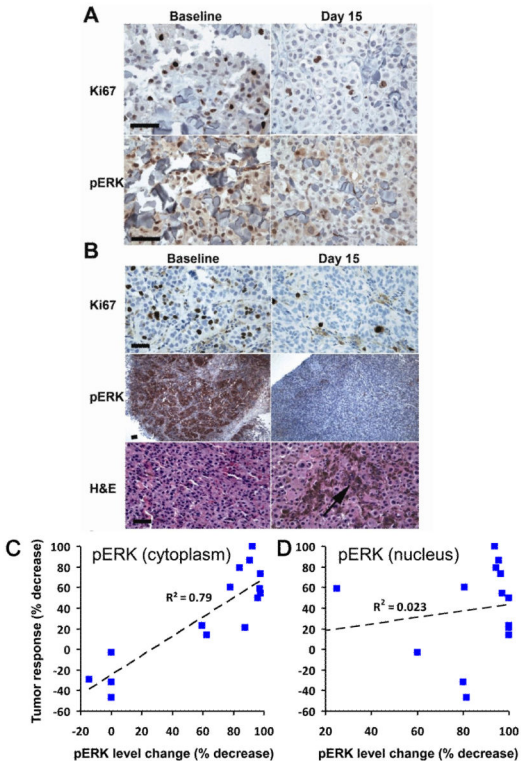

Fig 3. Semi-quantitative immunohistochemistry in paired tumor biopsies

Matched baseline and day 15 tumor samples are at the same magnification; the measurement bar is 70 μm.

A. Representative IHC for Ki67 and pERK staining is shown for patient 12.

B. Representative IHC for Ki67, pERK and H&E staining is shown for patient 42. The arrow indicates tumor breakdown with macrophages engulfing the released melanin in the day 15 sample.

C. Summary graph showing correlation of reduction in cytoplasmic pERK with tumor responses (data from Supplementary Table 2).

D. Summary graph indicating weak correlation of reduction in nuclear pERK with tumor responses.

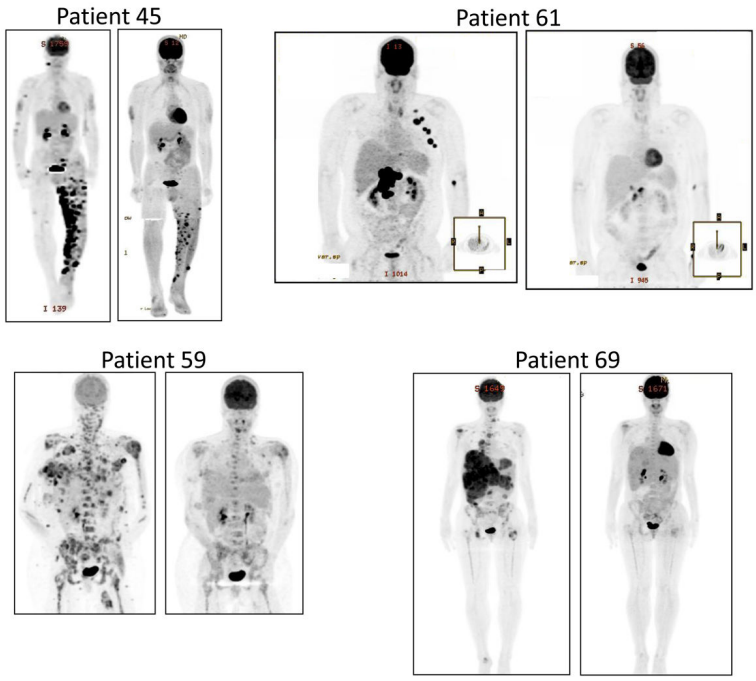

Fig 4. Representative PET scans for patients taken pre-dose and following 2 weeks of dosing with PLX4032

Each of these image pairs demonstrates significant reduction in FDG uptake following PLX4032 treatment. Note that tumor regressions were later documented for each of these patients: best responses were 70% for patient 45, 70% for patient 59, 68% for patient 61 and 37% for patient 69.